INVESTIGATION ON THE COMPRESSIVE STRENGTH OF GROUTED CLAY MASONRY WALLS

Domingues, P.(1); Corrêa, M.R.S.(2); Ramalho, M.A.(3)

ABSTRACT

This work deals with compressive strength of grouted clay masonry walls and its main purpose is to study the behaviour of grout and clay units as a whole. First, several results obtained from laboratory compressive tests are presented in order to evaluate the strength of walls from the strength of units, mortar and grout. Ten grouted walls, with two patterns of grouting, were tested under compressive loads. Besides, several compressive tests were also carried out in order to verify the strength of prisms, with two and three blocks, mortar, grout and clay units. Then, different relationships among strengths of components and walls were established. After that, the paper shows some results obtained from numerical modellings based on finite element analysis and the conclusions of the research.

Keywords: compressive strength; grouted walls; clay units; finite element; laboratory tests

(1) Graduate Student e-mail: patdg@sc.usp.br
(2) Senior Lecturer e-mail: correa@sc.usp.br
(3) Senior Lecturer e-mail: ramalho@sc.usp.br

São Paulo University – São Carlos Engineering School
Structures Engineering Department
Av. Dr. Carlos Botelho, 1465
CEP 13560-250 São Carlos, SP, Brazil

INTRODUCTION

Many different research projects have been developed on compressive strength of masonry walls throughout the world. It is not a surprise, because this is the most important characteristic of structural masonry. Those research studies have been made in order to reach a high level of economy and safety in the design of masonry buildings.

The ultimate compressive strength of masonry walls can be evaluated by three different ways. The first one is to consider separately the components. Then, units, mortar and eventually grout are tested and the results can be used to evaluate the strength of the wall as a whole. If the relationship between the strength of the components and the strength of the wall is well established, this proceeding can be a very interesting control process. Another procedure is testing two or three-block prisms. It is an interesting one because relevant information about masonry behaviour can be obtained doing simple tests that do not request sophisticated laboratory equipment. Obviously, those results are useful if reliable relationships between prisms and masonry strengths are already established. If it is not yet, the results obtained from prisms' tests won't be validated. The last way is the more trustful and reliable one, although the most expensive: testing full-scale walls. This test permits obtaining the ultimate capacity of masonry directly. The cost and difficulty in executing this procedure is its main problem. Also the laboratory apparatus is more sophisticated than that used for testing components or prisms. Those are factors that make the common use of this procedure impracticable.

In resume, it is easy to understand the importance of establishing reliable relationships among blocks, prisms and masonry strengths in order to design safe structures at a cost effective and fast way.

EXPERIMENTAL WORK

Test overview

Using 14x19x29 (cm) clay blocks, ten masonry walls (14x120x240,cm) were built with two different patterns of grouting distribution: Five four-grouted-hole walls and five six-grouted-hole walls. The main purpose was verifying the grout influence on the ultimate stress of wall and on its behaviour. The blocks used had 406 cm^2 of gross area and 203 cm^2 of net area. The bed joints were filled with 62% of the gross area, adopting a thickness of 10 mm.

A 1:0.5:4.5 mortar (cement: lime: sand, by volume) was used with a 1.0 water/cement (w/c) ratio. Grout was 1:0,05:2,2:2,4 (cement: lime: sand: fine gravel, by volume) with a 0.72 w/c ratio.

Ungrouted blocks were tested to characterize the average compressive strength of the set of blocks received. Also, grouted blocks, grout and mortar specimens, two and three-block prisms and walls were tested, see fig.1. The main results are shown in table 1.

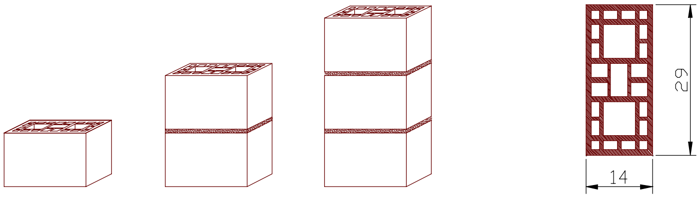

Figure 1. Prisms and blocks used in tests

Table 1. Specimens' quantities

Test	Specimens		Specimens' strength (MPa)
	Type	Characteristic	Mortar 1: 0.5: 4.5
			28 days
Compression	Block 14x19x29 (cm)	Ungrouted	12
		Grouted	18
	½ Block 14x14x19 (cm)	Ungrouted	11
	Grout	Cylinder (10x20 cm)	41
	Mortar	Cylinder (5 x 10 cm)	60
	Prism	2 blocks (14x19x40, cm)	18
		3 blocks (14x19x60, cm)	18
	Wall panels	14 x 120 x 240(cm)	8

Two test stages were adopted: the first one, with five walls with a 196 cm^2 grouted area, and the second one, with five walls with a 256 cm^2 grouted area, see Fig. 2 and 3.

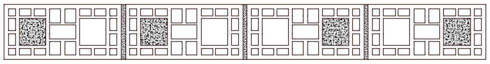

Figure 2. 1st test stage – 4 grouted holes

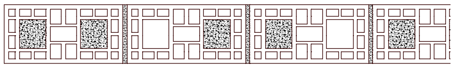

Figure 3. 2nd test stage – 6 grouted holes

Fig.4 shows the instrumentation used in the wall tests. In order to measure vertical shortenings, four transducers with 10-mm course, were used on the two faces. Another transducer with 50-mm course was placed perpendicular to one of the faces to measure displacements in that direction. Load was applied in a 20kN/min rate. Eleven ungrouted blocks, three grouted blocks and two mortar cylinders were also instrumented with transducers, aiming the measure of the Young modulus. A linear behaviour was adopted for blocks between 30% and 80% of failure load and up to 40% of failure load for the mortar cylinders.

Results

Fig. 5 to 13 and table 2 show the experimental results related to mortar, grout, blocks, prisms and walls failure stresses. It has to be pointed out that two wall tests were rejected because they were not centrally loaded.

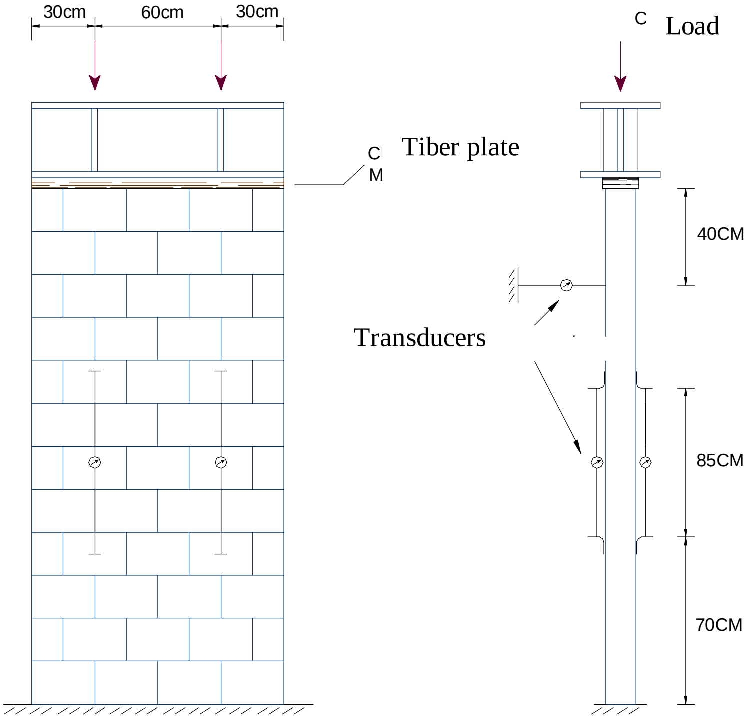

Figure 4. Instrumentation and loads on the wall

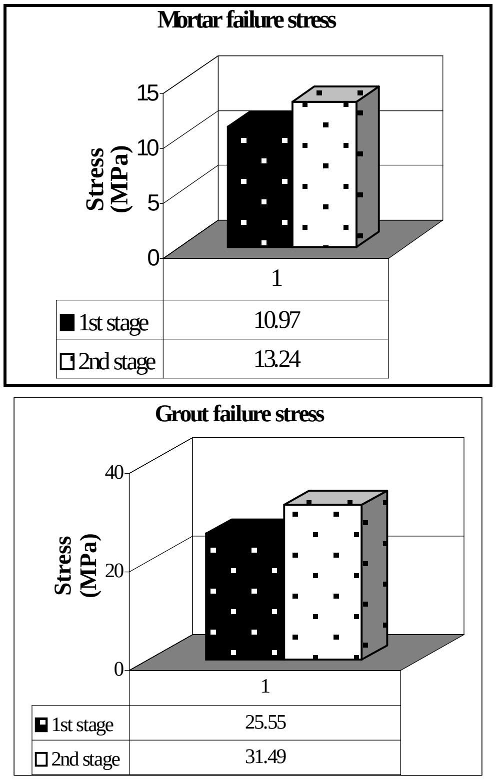

Figure 5. Mortar and grout specimens’ failure compressive stress

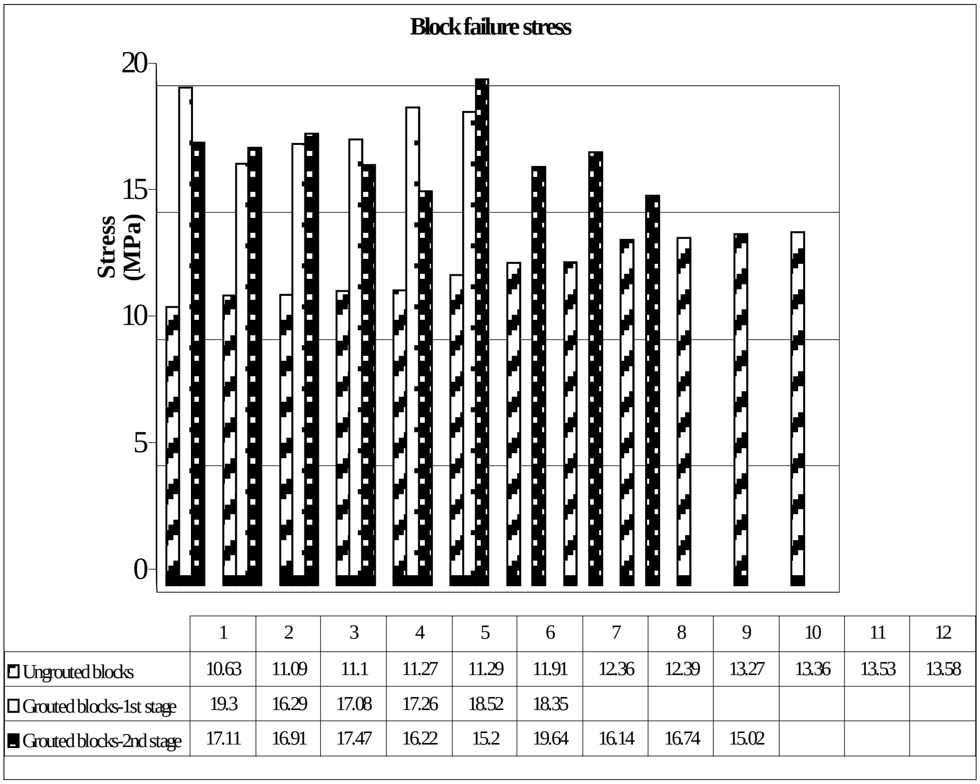

	1	2	3	4	5	6	7	8	9	10	11	12
◪ Ungrouted blocks	10.63	11.09	11.1	11.27	11.29	11.91	12.36	12.39	13.27	13.36	13.53	13.58
☐ Grouted blocks-1st stage	19.3	16.29	17.08	17.26	18.52	18.35						
■ Grouted blocks-2nd stage	17.11	16.91	17.47	16.22	15.2	19.64	16.14	16.74	15.02			

Figure 6. Ultimate blocks capacity

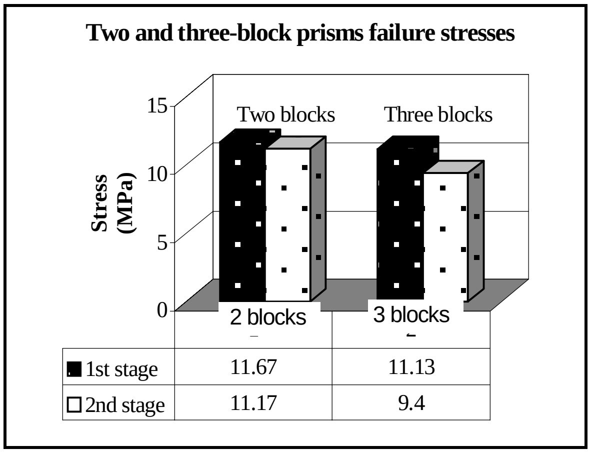

	2 blocks	3 blocks
■ 1st stage	11.67	11.13
☐ 2nd stage	11.17	9.4

Figure 7. Prisms failure compressive stress

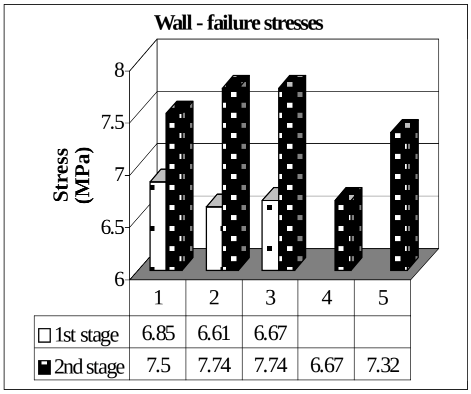

	1	2	3	4	5
□ 1st stage	6.85	6.61	6.67		
■ 2nd stage	7.5	7.74	7.74	6.67	7.32

Figure 8. Walls ultimate strength

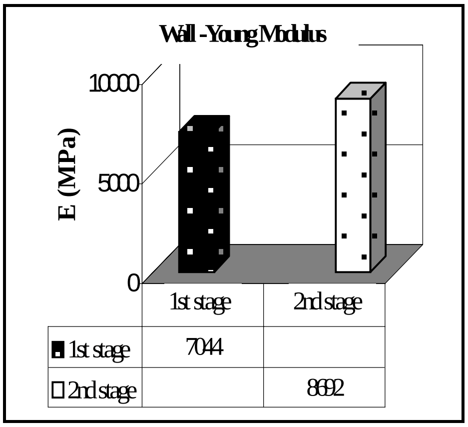

	1st stage	2nd stage
■ 1st stage	7044	
□ 2nd stage		8692

Figure 9. Walls average Young Modulus

Table 2. Mortar and block Young Modulus

Specimen	Young Modulus (MPa)
Ungrouted block	8172*
Grouted block	8493*
Mortar	10900*

* Values referred to net area

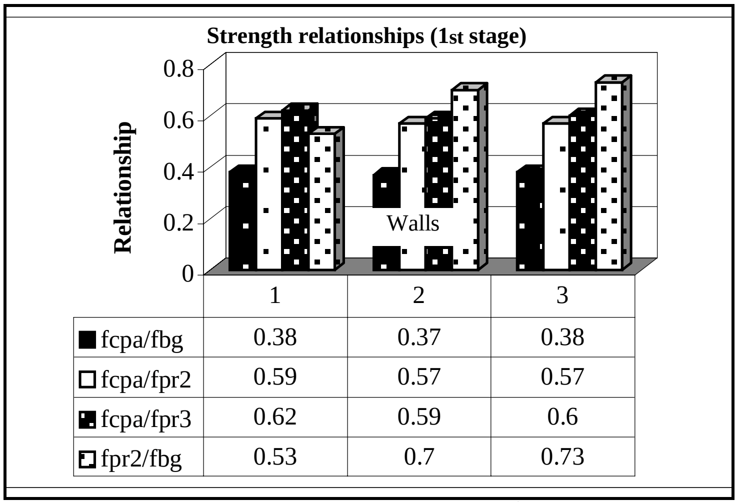

	1	2	3
■ fcpa/fbg	0.38	0.37	0.38
□ fcpa/fpr2	0.59	0.57	0.57
▨ fcpa/fpr3	0.62	0.59	0.6
▫ fpr2/fbg	0.53	0.7	0.73

Figure 10. Strength relationships – 1^{st} test stage

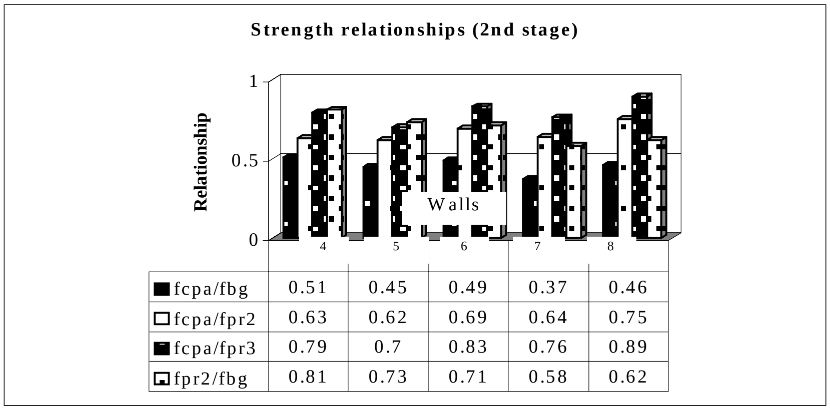

	4	5	6	7	8
■ fcpa/fbg	0.51	0.45	0.49	0.37	0.46
□ fcpa/fpr2	0.63	0.62	0.69	0.64	0.75
■ fcpa/fpr3	0.79	0.7	0.83	0.76	0.89
▣ fpr2/fbg	0.81	0.73	0.71	0.58	0.62

Figure 11. Strength relationships – 2nd test stage

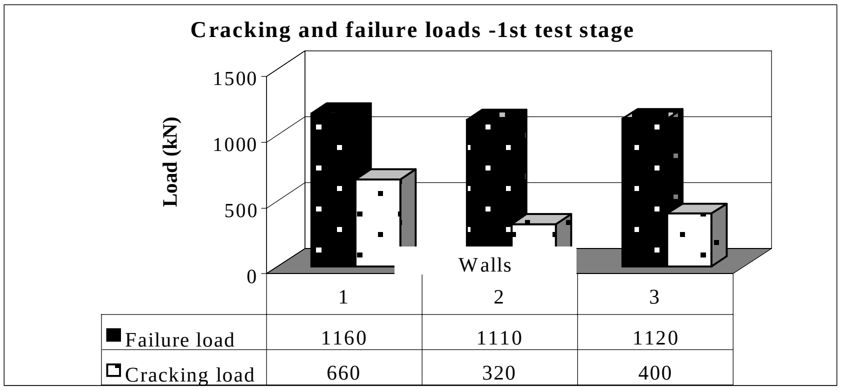

	1	2	3
■ Failure load	1160	1110	1120
□ Cracking load	660	320	400

Figure 12. Failure and cracking wall loads – 1st test stage

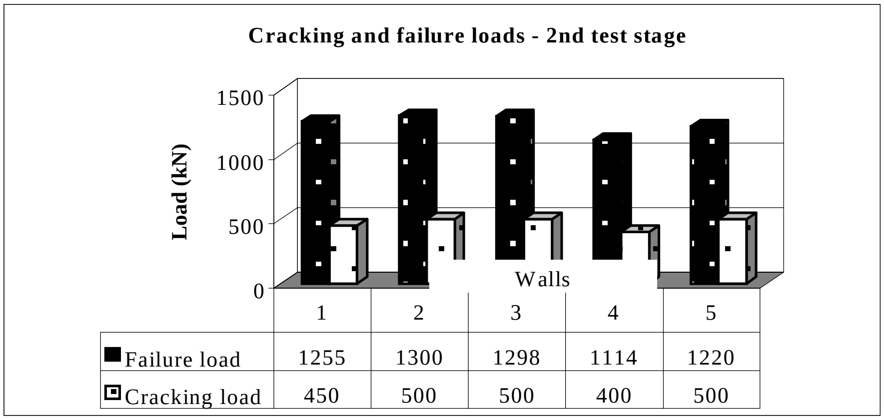

	1	2	3	4	5
■ Failure load	1255	1300	1298	1114	1220
▣ Cracking load	450	500	500	400	500

Figure 13. Failure and cracking wall loads – 2nd test stage

NUMERICAL MODELLING

Characteristics of the numerical models

Based on experimental results of the compression tests on walls and components, two finite element models were done to simulate the six-grouted-hole masonry walls (see Fig. 3). The software Ansys 5.5 [1] was used. The first one was a micro-model, simulating grouted, ungrouted blocks and mortar strips separately. The second one was based on the macro-modelling technique, using a homogeneous equivalent material for the entire wall. Table 3 shows values used in the models.

Table 3. Components' characteristics

Models	Materials	Characteristics	Panel Size
1	Ungrouted block	E_b=817 kN/cm^2 and ν_b=0.25	10.4x119x240
	Grouted blocks	E_{bg}=849 kN/cm^2 and ν_b=0.25	
	Mortar	E_m=1090 kN/cm^2 and ν_m= 0.20	
2	Grouted walls	E_{pa}= 1242 kN/cm^2 and ν_{pa}=0.25	10.4x119x240

The thickness of the elements in the model is 10.4cm, instead of the actual thickness of the block, 14cm. That is for maintaining the net/gross area ratio equal to 74%. The panels were simulated by membrane finite elements (PLANE 42 of Ansys). The nodes at the base were constrained in X and Y directions.

Results

Fig. 15 and 16 show some results corresponding to load of 300 kN. The stiffness in the 2nd model is higher than in the 1st one, since the displacements are lower in that case. Model 1 shows relevant differences between mortar and blocks stresses. Due to the restraint at the base, there are some deviations in the stresses. That fact drives to the appearance of compression stresses X in the horizontal direction (not presented here). Experimental and theoretical results corresponding to the shortenings measured by the transducers (see fig. 4) are shown in table 4, for the sake of comparison.

Displacement Y (cm)

Stress Y (kN/cm^2)

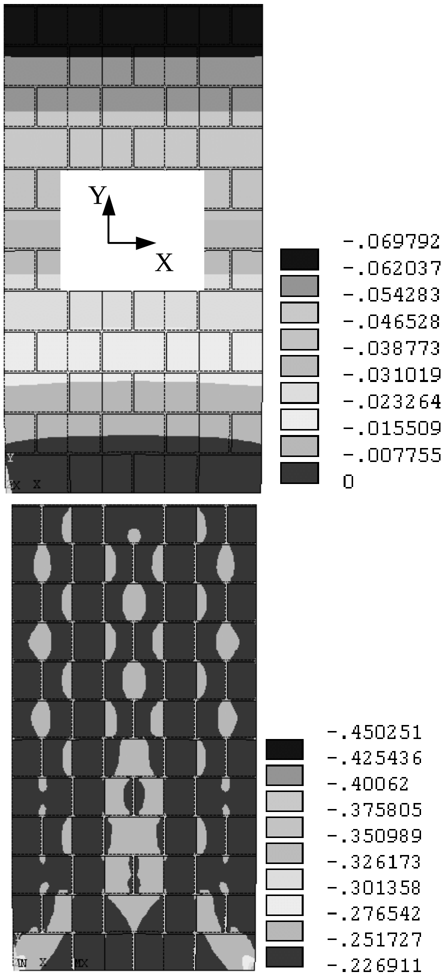

Figure 15. Contour curves – Model 1 – F=300 kN

Displacement Y (cm)

Stress Y (kN/cm^2)

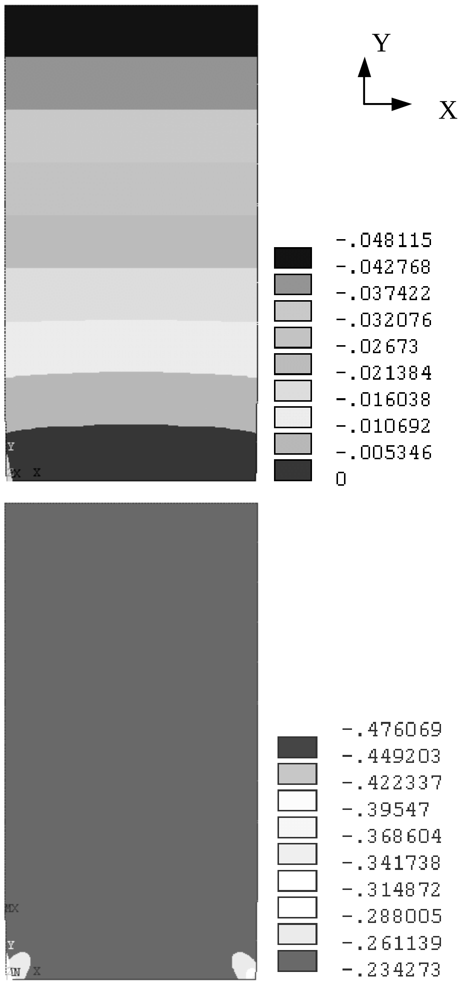

Figure 16. Contour curves – Model 2 – F=300 kN

Table 4. Comparison of numerical and experimental relative displacements

Wall	F=136 kN			F=300 kN			F=420 kN		
	Average shortenings (mm)			Average shortenings (mm)			Average shortenings (mm)		
	Exper.	Numeric		Exper.	Numeric		Exper.	Numeric	
		Model 1	Model 2		Model 1	Model 2		Model 1	Model 2
4	0.074	0.11	0.07	0.18	0.22	0.15	0.23	0.30	0.21
5	0.073			0.16			0.24		
6	0.073			0.17			0.23		
7	0.10			0.20			0.27		
8	0.080			0.18			0.24		
Average	0.080			0.18			0.24		

THEORETICAL ULTIMATE WALL CAPACITY EVALUATION

Failure loads were theoretically estimated (fig. 17), with the assumption that ultimate component strengths in the whole structure are the same as in the individual compressive tests. Those results should be the maximum load that panels could support.

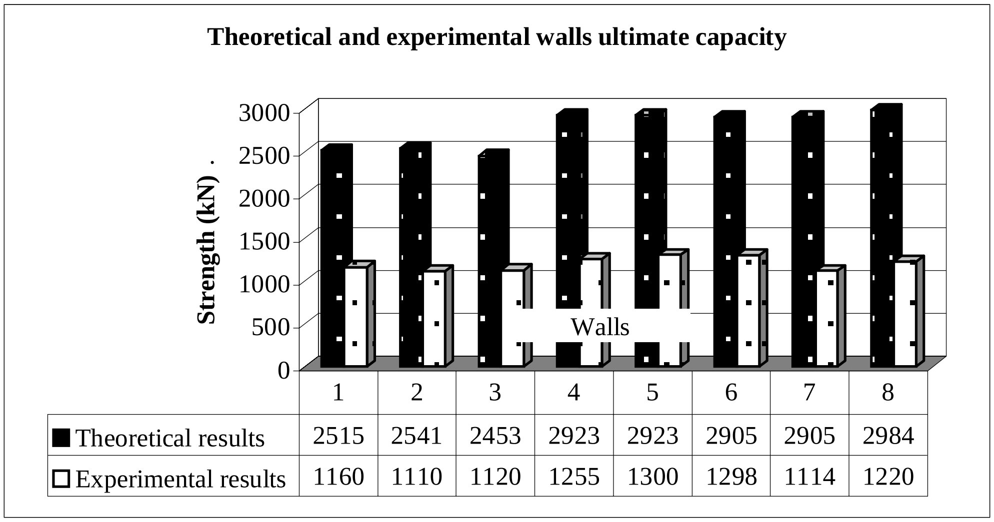

	1	2	3	4	5	6	7	8
■ Theoretical results	2515	2541	2453	2923	2923	2905	2905	2984
☐ Experimental results	1160	1110	1120	1255	1300	1298	1114	1220

Figure 17. Maximum ultimate loads of walls

ANALYSIS AND CONCLUSIONS

Experimental tests allowed developing wall analysis in terms of failure, cracking and stiffness behaviour. Relationships between strengths of blocks, prisms and wall were obtained and tests behaved as expected.

In terms of the strength results, it was found that:

i. The average failure stress of the walls, tested in the first stage, was 45% of the theoretical value; for the second stage of tests, it was 42%.
ii. According to a statistical analysis of wall stress results, it can be concluded that in accordance to t-Student test for independent samples, with 5% of significance, stress improvement happened due to improvement of grouted area.
iii. The average compressive strength of blocks was 12,15 MPa, while this value for half blocks reached 15,89 MPa. Higher stress variations happened with half blocks than with the entire blocks. Increasing the grouted area in nearly 10% led to a 50% growth of compressive strength of the walls.
iv. Cracking appeared at 41% and 38% of the ultimate load for the first and second test stages, respectively. It is worthy of note that for ungrouted walls the first crack appeared at 49% of the ultimate load. So, the groute did not modify the load of cracking for the walls.

As expected, the increase of the grouted area generated a more stiffened structure. The average Young modulus reached 6985 MPa and 8530 MPa in the first and second testing stages, respectively.

At last, some findings obtained from numerical modelling should be emphasized:

i. Due to displacement constraints in X and Y directions at wall base nodes, compression stresses developed in X direction, influencing structure behaviour. That fact can explain the absence of cracking near the base during the tests.

ii. In the first numerical model, stress concentration appeared under head joints. That fact can explain the appearance of cracking at those places in some tests.

iii. Comparing the 2nd and the 1st numerical models, it is easy to notice that the former one is stiffer. Experimental results are between the limits provided by the two alternative numerical models. (Fig. 18).

iv. Based on the obtained results, reasonable relationships between theoretical displacements (obtained from models 1 and 2) and experimental displacements can be established, as shown in Fig. 19.

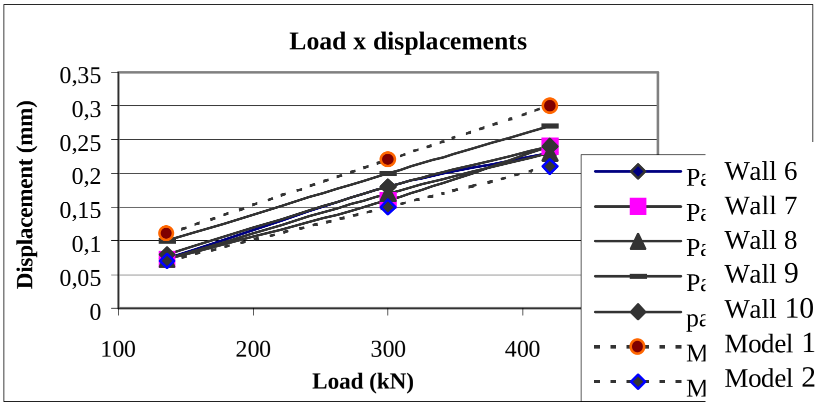

Figure 18. Load x displacement diagrams graph for three different loading stages (theoretical and experimental results)

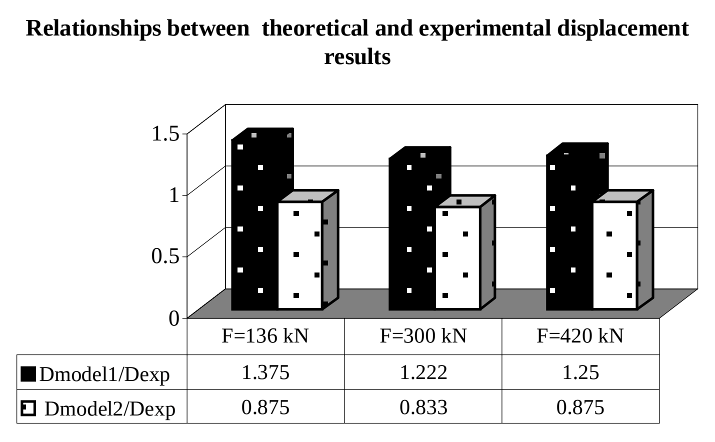

D_{model1} : 1st model displ., D_{model2}.: 2nd model displ., D_{exp} : Experimental displ.

Figure 19. Relationships between numerical and experimental displacement results

ACKNOWLEDGEMENTS

The authors gratefully acknowledge the support of the Brazilian research funding institutions CNPq - National Council for Scientific and Technological Development - and FAPESP - São Paulo State Research Support Foundation.

REFERENCES

ANSYS (1998). Manual - Version 5.5, Houston, USA.